Ginzburg-Landau theory of aqueous surfactant solutions

G. Gompper, Stefan Klein

Classification
Physics Abstracts
61.20G — 61.25E — 64.60C

Ginzburg-Landau theory of aqueous surfactant solutions

G. Gompper and Stefan Klein

Sektion Physik der Ludwig-Maximilians Universität München, 8000 München 2, Germany

(Received 26 May 1992, accepted 15 June 1992)

Abstract. — A simple two order-parameter Ginzburg-Landau theory for binary mixtures of water and amphiphile is introduced. The amphiphile concentration is described by a scalar, the orientational degrees of freedom of the amphiphile by a vector order parameter. Phase diagrams are calculated by minimizing the free energy functional. Several ordered lyotropic phases of lamellar, hexagonal, inverse hexagonal, and cubic structure exist. Phase diagrams show the sequence of ordered phases with increasing amphiphile concentration commonly observed in such systems. Several scattering intensities characterizing the disordered phase are calculated. They clearly show the tendency for bilayer or micelle formation. Finally, the elastic bending constants of surfactant bilayers are determined. The bending modulus κ is found to depend only on the orientational profile of a flat bilayer.

1. Introduction.

Aqueous surfactant solutions, i.e. mixtures of water and amphiphiles, show a large variety of unusual phenomena [1-4]. For example, for low surfactant concentrations a disordered phase is observed, in which the amphiphiles self-assemble into spherical and cylindrical micelles. Amphiphiles in aqueous solution can also assemble in bilayers and vesicles. At higher surfactant concentrations and low temperatures, several ordered lyotropic phases have been found, with lamellar, hexagonal and cubic symmetries. Here, the cubic phase with bicontinuous structure [5, 6] is of particular interest. At higher temperature, another disordered phase exits with a characteristic scattering behavior which is dominated by a broad peak at finite wavevector.

Due to this variety of interesting phenomena, and the importance of aqueous surfactant solutions in biology, these systems have been studied intensively over the last years, both experimentally and theoretically. On the theoretical side, various models have been proposed, each focusing on a different aspect of the amphiphilic system. The underlying mechanism, which is responsible for all these effects, is clear: polar molecules like water and polar head groups of amphiphiles want to avoid contact with the hydrocarbon chains of the amphiphile tails. This leads to the formation of micelles and bilayers in aqueous surfactant solutions. With increasing surfactant concentration these aggregates pack together to form the ordered lyotropic

phases. Due to the complexity of the system under consideration, drastic simplifications have to be made. "Lattice "models [7-10] simplify the two-particle interactions and discretize space, in order to facilitate a statistical analysis. "Interfacial "models [11-14] use bilayers as the basic building block. All the properties of the molecules and their interactions enter the model via the elastic bending energy [11] of bilayers. Finally, "thermodynamic"models [15] consider micelles as the basic units of the theory. Micelles of different sizes are considered to be in chemical equilibrium with each other and with amphiphiles in solution.

Each of these models has its disadvantages. In the "lattice"models, a realistic description of the ordered lyotropic phases is difficult. "Interfacial "models fail for weak amphiphiles. Furthermore, they cannot easily describe the coexistence of a phase made of bilayers, like a lamellar phase, and another one with a different structure, like the hexagonal phase. 'Thermodynamic' models are restricted to micelles.

In this paper, we introduce a Landau-Ginzburg model for aqueous surfactant solutions, which is inspired by Landau models for ternary oil-water-surfactant mixtures [16-19]. We will demonstrate that this model can account for a large part of the spectrum of phenomena in aqueous surfactant solutions. In section 2, the model is defined in detail. It is used in section 3 to calculate the scattering intensity of the homogeneous phases. In section 4, the phase diagrams and the structure of the ordered lyotropic phases are discussed. Section 5 is devoted to the study of micelles and bilayers. Finally, the elastic properties of bilayers are calculated in section 6.

2. Ginzburg-Landau model.

In order to construct a Ginzburg-Landau model for water-surfactant mixtures, one has to decide first which degrees of freedom of the system are considered to be essential and therefore have to be included in the model. Obviously, a scalar order parameter field, $\phi(\mathbf{r})$, for the local density difference of the two components is necessary, as in any other binary fluid mixture. To describe the anisotropy of the surfactant molecules, we introduce a vector order parameter field, $\tau(\mathbf{r})$, which models the orientation of the amphiphiles [7-10, 18, 19].

Let us consider first a binary fluid mixture of two ordinary fluids, with isotropic interactions between all molecules. Its free energy is given by

$$\mathcal{F}_{\text{bin}} = \int \mathrm{d}^3 r[\beta_1(\nabla\phi)^2 + f_1(\phi) - \mu\phi] \tag{1}$$

where μ is the chemical potential difference between the two components. $f_1(\phi)$ is the free energy density of *homogeneous* order parameter configurations; its form will be specified below. Here, the gradient term, with $\beta_1 > 0$, disfavors spatially varying order parameter configurations. We consider next a pure amphiphile system. In this case spatially modulated phases, like a smectic liquid crystalline phase, do exist. This can be modelled in a Ginzburg-Landau theory by a negative gradient term, which favors spatial modulations. Higher order derivatives are then necessary to make the model thermodynamically stable. Thus, for pure amphiphile we have the free energy functional

$$\mathcal{F}_{\text{amph}} = \int \mathrm{d}^3 r[\alpha_1(\nabla\cdot\tau)^2 + \alpha_2(\nabla^2\tau)^2 + \alpha_3(\nabla\times\tau)^2 + \alpha_4(\nabla(\nabla\cdot\tau))^2 + f_2(\tau^2)] \tag{2}$$

with $\alpha_1 < 0$ to describe the tendency of the amphiphilic molecules to put their heads or their tails together, and $\alpha_2 > 0$, $\alpha_4 > 0$ to insure thermodynamic stability. Here, we have included

all terms with first and second derivatives, which are rotationally invariant and are quadratic in the order parameter. Note that a term $(\nabla\tau)^2 = \sum_{i,j}(\partial_i\tau_j)(\partial_i\tau_j)$ does not appear, because by partial integration it can be shown that this term is equivalent to a linear combination of other terms in (2) (in case the boundary contributions can be neglected). Finally, the amphiphiles in aqueous solution are oriented in such a way that the polar heads point towards the water. This anisotropic interaction is described by terms containing both order parameters. We include again all terms with first and second derivatives, which are quadratic in the order parameters. This is, in fact, only a single term, so that we finally arrive at

$$\begin{aligned}\mathcal{F} = \int \mathrm{d}^3r[&\alpha_1(\nabla\cdot\tau)^2 + \alpha_2(\nabla^2\tau)^2 + \alpha_3(\nabla\times\tau)^2 \\ &+ \alpha_4(\nabla(\nabla\cdot\tau))^2 + \beta_1(\nabla\phi)^2 + \gamma(\tau\cdot\nabla\phi) + U(\phi,\tau^2) - \mu\phi]\end{aligned} \tag{3}$$

To complete the definition of our free energy functional, we need to specify the free energy density $U(\phi,\tau^2)$ of homogeneous order parameter configurations. We consider here two different forms for this function, which are derived from different principles. The first is an expansion in powers of the order parameters, which makes our model a true Ginzburg-Landau theory, where all powers allowed by symmetry appear, so that

$$U(\phi,\tau^2) = f_1(\phi) + \bar{b}_2\tau^2 + \bar{b}_4\tau^4 + \bar{c}_1\phi\tau^2 + \bar{c}_2\phi^2\tau^2 \tag{4}$$

with

$$f_1(\phi) = \sum_{n=2,6} \bar{a}_n\phi^n \tag{5}$$

The coefficients in (5) are chosen in such a way that *two* minima exist; we have to go to a sixth order polynomial because we want to break the symmetry between the two phases at coexistence. To ensure thermodynamic stability, $\bar{a}_6 > 0$, $\bar{b}_4 > 0$ and $\bar{c}_2 > 0$. We take $\bar{b}_2 > 0$ so that no homogeneous phases with non-zero orientation ("nematic ") can exist. The term $\bar{c}_1\tau^2\phi$ acts like a local chemical potential, which favors locally large surfactant concentrations ϕ where τ^2 is large for $\bar{c}_1 < 0$.

The second possibility is to obtain the free energy functional as a sum of interaction energy and entropy. With pairwise interactions, the energy contributions to the free energy density $U(\phi,\tau^2)$ are terms proportional to ϕ^2 and τ^2. The entropy is calculated in the random mixing approximation. It is shown in Appendix A that this gives the generalized Flory-Huggins form

$$S(\phi,\tau^2) = -\int \mathrm{d}^3r\,[\phi\ln\phi + M(1-\phi)\ln(1-\phi) + \phi\,(c_2\tilde{\tau}^2 + c_4\tilde{\tau}^4 + ..)] \tag{6}$$

where $\tilde{\tau} = \tau/\phi$ is the average local orientation of the amphiphiles at fixed concentration, and M is the relative molecular volume of the amphiphile (compared to water). In this case we have

$$U(\phi,\tau^2) = f_1(\phi) + b_2\tau^2 + T\phi\,[c_2\tilde{\tau}^2 + c_4\tilde{\tau}^4] \tag{7}$$

with

$$f_1(\phi) = a_2\phi^2 + T[\phi\ln\phi + M(1-\phi)\ln(1-\phi)] \tag{8}$$

For $\tau = 0$, $U(\phi,\tau^2 = 0) = f_1(\phi)$ is identical with the usual Flory-Huggins form [20] of the free energy.

In equations (7) and (8), we have introduced a temperature T for the case of the Flory potential. For the Landau potential (4), a temperature can be defined analogously, i.e. by

writing the potential $U(\phi,\tau^2)$ in the form $[a_2\phi^2 + b_2\tau^2 - TS(\phi,\tau^2)]$. Thus, in equations (4), (5) we set $\bar{a}_2 = a_2 + \tilde{a}_2 T$, $\bar{b}_2 = b_2 + \tilde{b}_2 T$, and $\bar{a}_j = \tilde{a}_j T$, $\bar{b}_j = \tilde{b}_j T$ for $j > 2$, as well as $\bar{c}_j = \tilde{c}_j T$ for $j = 1, 2$. We will calculate phase diagrams as a function of the parameter T in sections 3 and 4 below. However, it has to be kept in mind that T cannot be easily compared with the temperature of a real system. The reason is that we have not taken into account all degrees of freedom in our model. In particular the rotational degrees of freedom of the water molecules have been shown to be important [21]. These degrees of freedom are considered to be integrated out in our model. The price we have to pay is that the interaction constants in our model become themselves temperature dependent. We will ignore this additional temperature dependence here. Thus, our results can be compared with experimental data only at constant temperature, as a function of the amphiphile concentration.

3. Scattering intensity of disordered phases.

We calculate the phase diagram of our model by minimizing the free energy functional (3) with respect to all order parameter configurations. The simplest phase is a homogeneous and isotropic disordered phase, in which the order parameter field $\phi(\mathbf{r})$ is constant, and $\tau(\mathbf{r})$ vanishes identically. Information about the order parameter correlations in this phase can be obtained from neutron or X-ray scattering experiments. We calculate the structure functions here in the Ornstein-Zernike approximation. To do so, we expand the free energy functional to second order in the deviations of the order parameters from their average values $\tau = 0$ and $\phi = \phi_0$. This is most easily done in Fourier space, with the result

$$\mathcal{F} = F_{\mathrm{MF}}(\phi_0) + \int \mathrm{d}^3k \begin{pmatrix} \tau_{\mathbf{k}} \\ \phi_{\mathbf{k}} \end{pmatrix} L(\mathbf{k}) \begin{pmatrix} \tau_{-\mathbf{k}} \\ \phi_{-\mathbf{k}} \end{pmatrix} + .. \tag{9}$$

where the matrix L is given by

$$L(\mathbf{k}) = \begin{pmatrix} K(\mathbf{k}) & -\frac{1}{2}\gamma\mathbf{k} \\ \frac{1}{2}\gamma\mathbf{k}^T & p^{-1}(\mathbf{k}) \end{pmatrix} \tag{10}$$

with

$$\begin{aligned} K_{jl} &= \zeta\delta_{jl} + \epsilon\frac{k_j k_l}{k^2} \qquad j,l \in \{1,2,3\} \\ p^{-1} &= \beta_1 k^2 + \frac{1}{2}\partial_\phi^2 U(\phi,\tau^2)|_{\phi=\phi_0,\tau=0} \end{aligned} \tag{11}$$

and

$$\begin{aligned} \zeta &= \alpha_3 k^2 + \alpha_4 k^4 + \frac{1}{2}\partial_\tau^2 U(\phi,\tau^2)|_{\phi=\phi_0,\tau=0} \\ \epsilon &= (\alpha_1 - \alpha_3)k^2 + \alpha_2 k^4 \end{aligned} \tag{12}$$

The inverse of the matrix L contains all structure functions. In particular, we find

$$< \phi(\mathbf{k})\phi(-\mathbf{k}) > = \frac{p(\zeta+\epsilon)}{\zeta + \epsilon - \frac{\gamma^2}{4}pk^2} \tag{13a}$$

$$< \tau(\mathbf{k}) \cdot \tau(-\mathbf{k}) > = \frac{2}{\zeta} + \frac{1}{\zeta + \epsilon - \frac{\gamma^2}{4}pk^2} \tag{13b}$$

$$< \tau_z(\mathbf{k})\tau_z(-\mathbf{k}) > = \frac{1}{\zeta + \epsilon - \frac{\gamma^2}{4}pk^2}\left[1 + \frac{\sin^2\theta}{\zeta}\left(\epsilon - \frac{\gamma^2}{4}pk^2\right)\right] \tag{13c}$$

where $\cos^2\theta = k_z^2/k^2$, so that θ is the angle between $\mathbf{k}$ and the z-axis.

We begin the discussion of this result with the case of the pure amphiphile system, for which $p(\mathbf{k}) = 0$. For the Flory free energy density (7), (8) this is the case for $\phi_0 = 1$. It is instructive to study the correlation function $< \tau_z(\mathbf{k})\tau_z(-\mathbf{k}) >$ as a function of the angle θ, see figure 1: for $\theta = \pi/2$, this correlation function is the conditional probability to find two amphiphiles oriented in the z-direction, when the vector joining the two is perpendicular to the z-axis. It can be shown easily with equation (13c) that for $\alpha_3 > 0$ (and $\alpha_4 > 0$), this function has its maximum always at $k = 0$. This reflects the tendency of the amphiphiles to self-assemble in monolayers: nearest neighbor molecules within a monolayer are oriented in the same direction. The correlation function for $\theta = 0$, on the other hand, describes the correlation along the axis of orientation. In this case, we observe an "antiferromagnetic "ordering on short length scales, corresponding to a tendency for the formation of surfactant *multi*-layers. The structure function (13c) has a peak at non-zero wave-vectors, as long as $\alpha_1 < 0$.

The real space correlations can be obtained from (13) by Fourier transform. They are shown in figure 2, and illustrate again the physics of self-assembly discussed above. The correlation

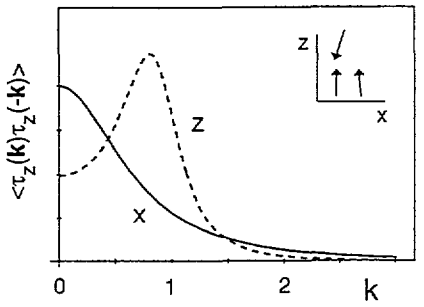

Fig. 1. — Correlation functions in Fourier space, $< \tau_z(k_x)\tau_z(-k_x) >$ (solid line) and $< \tau_z(k_z)\tau_z(-k_z) >$ (dashed line), for $\alpha_1 = -2$, $\alpha_2 = 0.5$, $\alpha_3 = 1.1$, $\alpha_4 = 0.2$, and $\partial_\tau^2 U|_{\tau=0} = 1$.

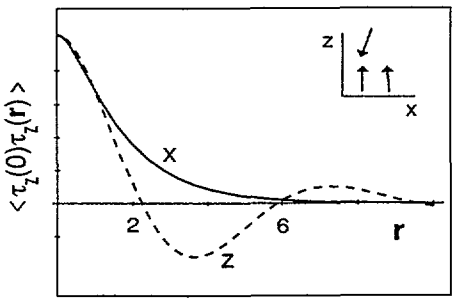

Fig. 2. — Correlation functions in real space, $< \tau_z(0)\tau_z(x) >$ (solid line) and $< \tau_z(0)\tau_z(z) >$ (dashed line). The parameters are the same as in figure 1.

function in the z-direction, integrated over the x- and y-coordinates, has the form

$$< \tau_z(z)\tau_z(0) >= A_z e^{-z/\xi_{z+}} \sin(\frac{z}{\xi_{z-}} + \psi_z) \tag{14}$$

where

$$\xi_{z\pm} = \sqrt{4(\alpha_2 + \alpha_4)/(D_z \pm \alpha_1)} \tag{15}$$

with

$$D_z = \sqrt{2(\alpha_2 + \alpha_4)\partial_\tau^2 U} \tag{16}$$

and $\cos\ \psi_z = \xi_{z-}/\sqrt{\xi_{z+}^2 + \xi_{z-}^2}$. It decays with exponentially damped oscillations, as long as $\alpha_1 < D_z$, whereas it decays monotonically for $\alpha_1 > D_z$. The line $\alpha_1 = D_z$ is called a disorder line [22, 23]. We are interested here only in the case $\alpha_1 < D_z$, because in this case the amphiphile-amphiphile interaction is such as to favor bilayer formation. The wave-length of the oscillations, ξ_{z-}, can be interpreted as the average thickness of a bilayer. The correlation function in the x-direction, integrated over the y- and z-coordinates, is found to be

$$< \tau_z(x)\tau_z(0) >= A_x e^{-x/\xi_{x+}} \sinh(\frac{x}{\xi_{x-}} + \psi_x) \tag{17}$$

where

$$\xi_{x\pm} = \sqrt{4\alpha_1/(\alpha_3 \pm D_x)} \tag{18}$$

with

$$D_x = \sqrt{2\alpha_4 \partial_\tau^2 U} \tag{19}$$

and $\cosh \psi_x = \xi_{x-}/\sqrt{\xi_{x+}^2 + \xi_{x-}^2}$. This correlation function decays exponentially, with no oscillations for $\alpha_3 > D_x$, whereas it starts to oscillate for $\alpha_3 < D_x$. Here, another disorder line occurs. For $\alpha_3 < D_x$ the correlations become quite complicated. We will always stay on the "monotonic"side of this disorder line. Note that the length scales in the x- and z-directions are different, and their ratio can be varied over a wide range by an appropriate choice of interaction parameters.

When water is added to the system, and the interaction between water and amphiphile is weak, the phase diagram is usually dominated by a miscibility gap between a water-rich and a surfactant-rich phase, both of which are disordered phases. The phase-diagram for such a case is shown in figure 3. We can now compare the scattering intensities within the two phases at coexistence. They are shown in figure 4 for $T = 0.5$. We find that the L_1-phase behaves like an ordinary binary liquid mixture: the scattering intensity $< \phi(\mathbf{k})\phi(-\mathbf{k}) >$ has a peak at $k = 0$, and $< \tau_z(\mathbf{k})\tau_z(-\mathbf{k}) >$ is essentially independent of the angle θ. We conclude that in this phase the amphiphiles do not form aggregates, the fluid is disordered on a molecular scale. In the L_2-phase, on the other hand, the fluid is strongly structured, as indicated by the scattering peaks at non-zero wavevector of all correlation functions, except $< \tau_z(\mathbf{k})\tau_z(-\mathbf{k}) >$ for θ near $\pi/2$. This demonstrates that self-assembly has set in, although the phase is still homogeneous on a macroscopic scale.

The scattering behavior *above* the critical temperature T_c is also interesting. The position of the scattering peak of the correlation functions $< \phi(\mathbf{k})\phi(-\mathbf{k}) >$ and $< \tau_z(k_z)\ \tau_z(-k_z) >$ as a function of the amphiphile concentration is shown in figure 5. It can be seen that the amphiphiles are *always* oriented antiferromagnetically along their axis of orientation, leading to a peak at finite wavevector for all surfactant concentrations. The peak position is essentially independent of surfactant concentration. A peak at finite k in the density-density correlation

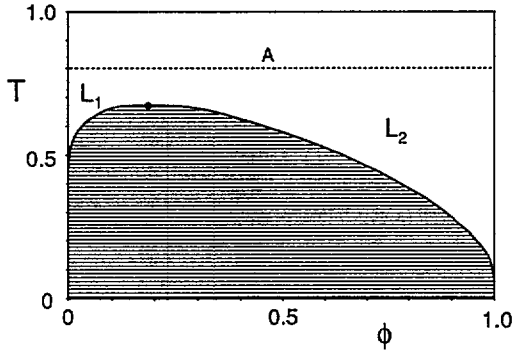

Fig. 3. — Phase diagram for the Flory free energy with the parameters $\alpha_1 = -6$, $\alpha_2 = 9$, $\alpha_3 = 5$, $\alpha_4 = 5$, $\beta_1 = 10$, $\gamma = 10$, $M = 20$, $a_2 = 1$, $b_2 = -10$, $c_2 = 17/12$. The dot (•) marks the position of the critical point.

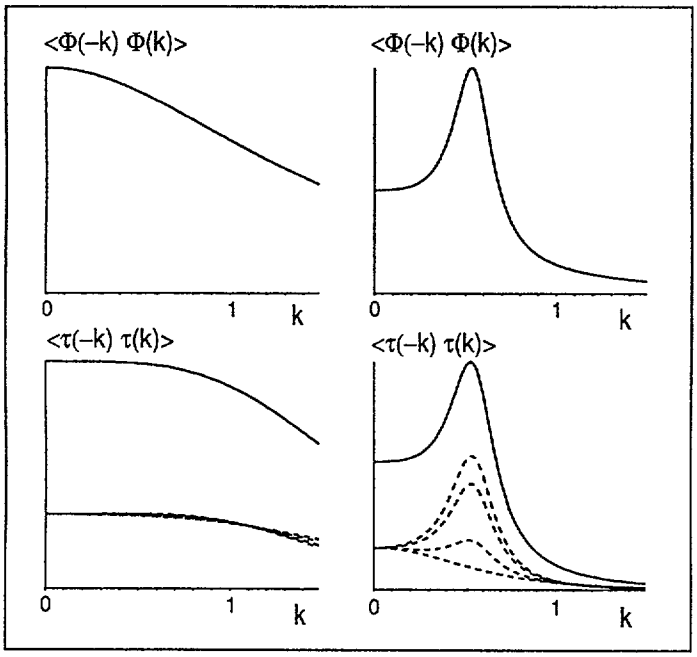

Fig. 4. — Correlation functions in Fourier space at two-phase coexistence, for the temperature $T = 0.5$ in figure 3. The curves on the left show the correlations in the water-rich L_1-phase, the curves on the right in the surfactant-rich L_2-phase. The dashed lines are the $< \tau_z(\mathbf{k})\tau_z(-\mathbf{k}) >$ correlations for $\Theta = 0$ (strongest peak at finite k), $\Theta = \pi/6$, $\Theta = 2\pi/6$, and $\Theta = \pi/2$ (peak at $k = 0$). The parameters are the same as in figure 3.

function, on the other hand, appears only at large surfactant concentrations. It does not move out continuously from $k = 0$, but appears suddenly at $k \simeq 0.4$. Furthermore, there is a range of amphiphile concentrations, where $< \phi(\mathbf{k})\phi(-\mathbf{k}) >$ has *two* peaks, one at $k = 0$, the other at finite k. This indicates a structure with *three* different length scales: (i) there is a bilayer-type structure with a repeat distance λ, which determines the peak position at non-zero $k \simeq k_{bl} = 2\pi/\lambda$ of *both* correlation functions ; (ii) this bilayer structure decays with a correlation length ξ_{bl}, which is inverse proportinal to the width of the peak at k_{bl}; (iii) there are density fluctuations, which decay with another correlation length ξ_ϕ, which is inverse proportional to the width of the peak at $k = 0$. The density-density correlation function looses its peak at $k = 0$ at a Lifshitz-line, which is given implicitly by

$$\gamma^2 = 2\beta_1 \partial_\tau^2 U(\phi, \tau^2)|_{\phi=\phi_0, \tau=0}. \tag{20}$$

At this line, the peak at $k \simeq k_{bl}$ already dominates the scattering intensity, so that the Lifshitz-line is of minor relevance here. Thus, at very large amphiphile concentrations, the density fluctuations become neglibible compared to the 'bilayer' fluctuations.

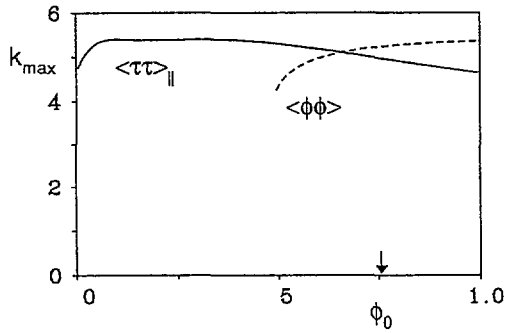

Fig. 5. — Concentration dependence of the peak positions of the scattering intensities $< \tau_z(k_z)\tau_z(-k_z) >$ (full line) and $< \phi(\mathbf{k})\phi(-\mathbf{k}) >$ (dashed line) along the path A in figure 3.

4. Phase diagrams - Ordered phases.

When the strength of the water-amphiphile and the amphiphile-amphiphile interaction is large enough, ordered phases can become stable in our model. We look again for configurations which minimize the free energy functional (3). Only crystalline phases with mirror symmetry will be considered here. In this case, it can be shown easily that $\nabla \times \tau \equiv 0$, and the vector field $\tau(\mathbf{r})$ can be obtained as the gradient [24] of a scalar field, $\Xi(\mathbf{r})$. Both order parameter fields are expanded in a Fourier series,

$$\begin{aligned} \phi(\mathbf{r}) &= \phi_0 + \sum_{i=1}^{N} \sum_{\mathbf{k} \in B_i} \phi_{\mathbf{k}} \cos(\mathbf{k} \cdot \mathbf{r}) \\ \Xi(\mathbf{r}) &= \sum_{i=1}^{N} \sum_{\mathbf{k} \in B_i} \Xi_{\mathbf{k}} \cos(\mathbf{k} \cdot \mathbf{r}) \end{aligned} \tag{21}$$

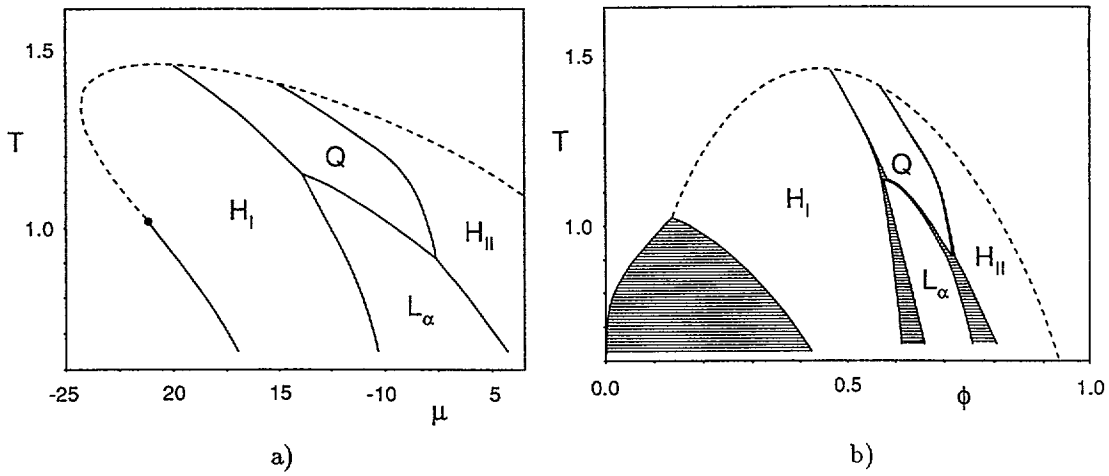

Fig. 6. — Phase diagram for the Flory free energy with the parameters $\alpha_1 = -6$, $\alpha_2 + \alpha_4 = 10$, $\beta_1 = 10$, $\gamma = 30$, $M = 20$, $a_2 = 1$, $b_2 = -10$, $c_2 = 17/12$, $c_4 = 1$. (a) Temperature *vs.* chemical potential plane. Phase transitions along dashed lines are second order. The tricritical point is marked by a dot (•). (b) Temperature *vs.* amphiphile concentration plane.

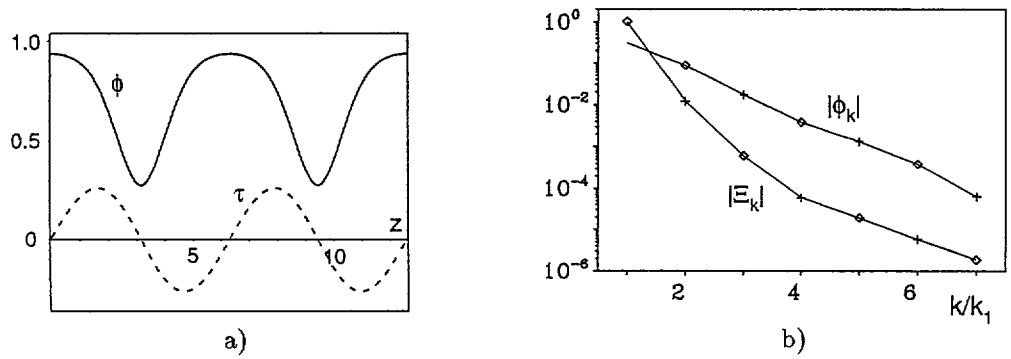

Fig. 7. — Order parameter profiles for the lamellar phase (L_α) at $T = 0.75$, $\mu = -7.5$ of figure 6, with lattice constant $a = 8.235$ and average amphiphile concentration $\phi_0 = 0.703$. (a) Real space profiles $\phi(z)$, $\tau_z(z)$. (b) Fourier amplitudes ϕ_k and Ξ_k; the crosses (+) indicate positive, the diamonds (◇) negative amplitudes. k_1 is the magnitude of the shortest wavevector.

where B_i denotes the i-th shell of reciprocal lattice vectors. The true minimum of the free energy is of course obtained for $N \to \infty$. The convergence of the series is in general quite good for all types of structures presented below. Our results are all obtained with $N = 6$, so that we have $2N + 2 = 16$ variational parameters (the Fourier amplitudes plus the lattice constant) [25].

A typical phase diagram for the Flory free energy density (7), (8) is shown in figure 6. It contains four types of ordered phases. The simplest phase is the lamellar phase (L_α), a stack of surfactant bilayers, which are separated by water layers. Its order parameter distribution is shown in figure 7. Remember that in our model ϕ is the amphiphile concentration. The

hexagonal phase (H_I) is a two-dimensional array of cylindrical micelles (of infinite length). Its structure, as obtained from our model, is shown in figure 8. Similarly, the inverse hexagonal [26] phase (H_{II}) is a two-dimensional array of water cylinders, separated by surfactant sheets, see figure 9. We have also found a stable simple cubic (sc) bicontinuous [13, 27] phase, with a structure shown in figure 10. Other cubic bicontinuous phases [13] may also be stable or metastable, but, due to the high numerical effort, have not been tested yet.

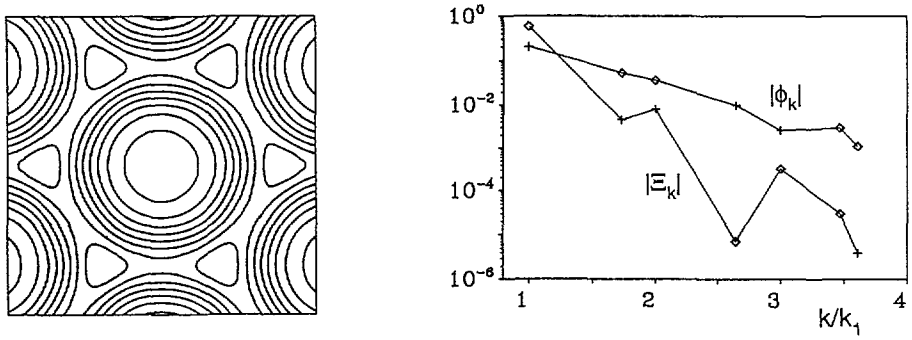

Fig. 8. — The order parameter distribution of the hexagonal phase (H_I) at $T = 0.75$, $\mu = -12.5$ of figure 6, with lattice constant $a = 9.386$ and average amphiphile concentration $\phi_0 = 0.562$. (a) Contour plot of the amphiphile density distribution. (b) Fourier amplitudes ϕ_k and Ξ_k; the crosses (+) indicate positive, the diamonds (◇) negative amplitudes. k_1 is the magnitude of the shortest wavevector.

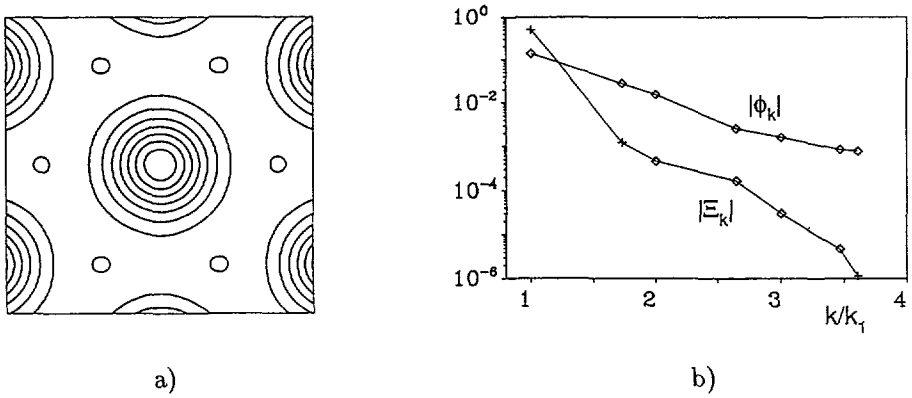

Fig. 9. — The order parameter distribution of the inverse hexagonal phase (H_{II}) at $T = 0.75$, $\mu = -5.0$ of figure 6, with lattice constant $a = 9.527$ and average amphiphile concentration $\phi_0 = 0.781$. (a) Contour plot of the amphiphile density distribution. (b) Fourier amplitudes ϕ_k and Ξ_k; the crosses (+) indicate positive, the diamonds (◇) negative amplitudes. k_1 is the magnitude of the shortest wavevector.

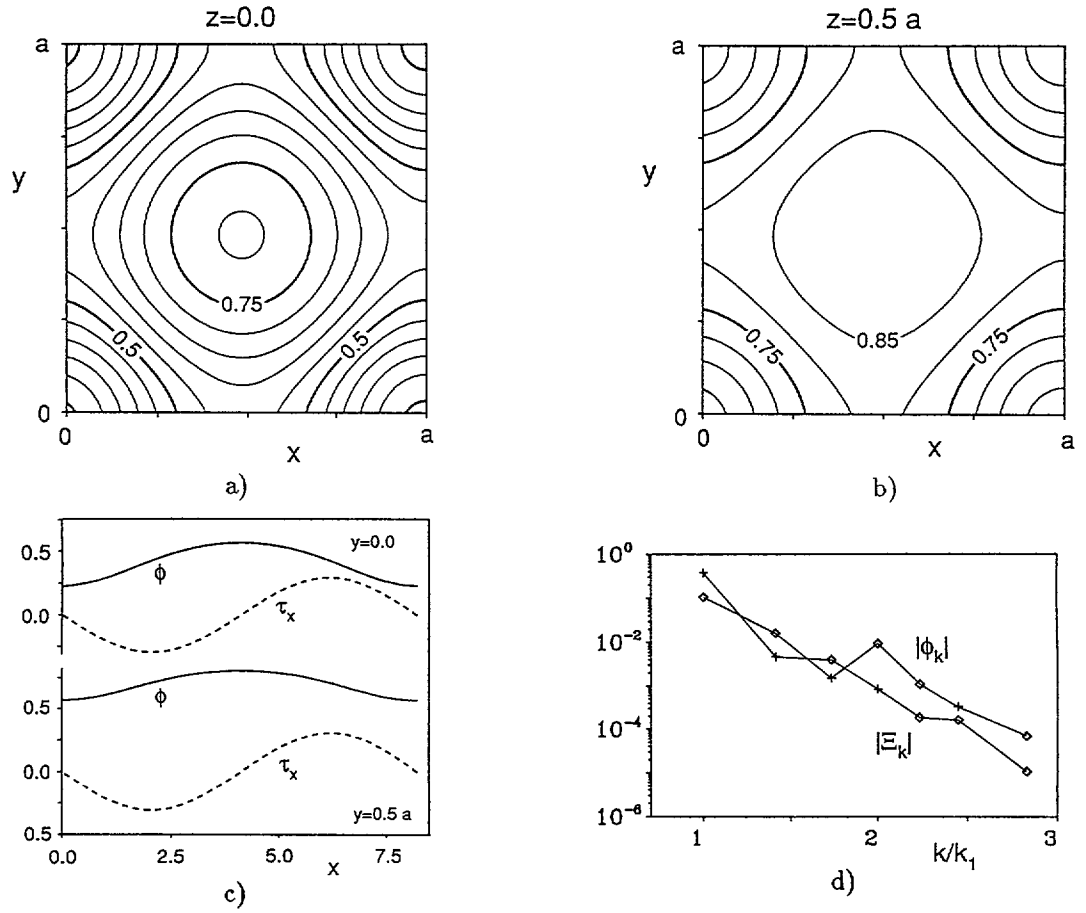

Fig. 10. — The order parameter distribution of the cubic (bicontinuous) phase (Q) at $T = 1.0$, $\mu = -9.0$ of figure 6, with lattice constant $a = 8.217$ and average amphiphile concentration $\phi_0 = 0.685$. (a) Contour plot of the amphiphile density distribution in the plane $z = 0$. (b) Contour plot of the amphiphile density distribution in the plane $z = a/2$. (c) Order parameter profiles $\phi(x)$ and $\tau_x(x)$ for $y = 0$, $z = 0$ and $y = a/2$, $z = 0$. (d) Fourier amplitudes ϕ_k and Ξ_k; the crosses (+) indicate positive, the diamonds (◇) negative amplitudes. k_1 is the magnitude of the shortest wavevector.

When the coupling constant $\alpha_1 < 0$ is increased in magnitude from $\alpha_1 = -6$ to $\alpha_1 = -10$, the inverse hexagonal phase is no longer present in the phase diagram, see figure 11. Furthermore, the pure amphiphile system is now in an ordered (cubic) phase at low temperatures.

Finally, we have also calculated the phase diagram for the Landau free energy density (4), (5), in order to see how strongly the phase diagram depends on the choice of the free energy density $U(\phi, \tau^2)$. The result is shown in figure 12. The most striking difference to the previous phase diagrams is that at low temperatures there is a re-entrant behavior from the cubic to the inverse hexagonal and back to the cubic phase with increasing surfactant concentration. The general phase behavior, however, is in agreement with the behavior found with the Flory free energy density (7), (8).

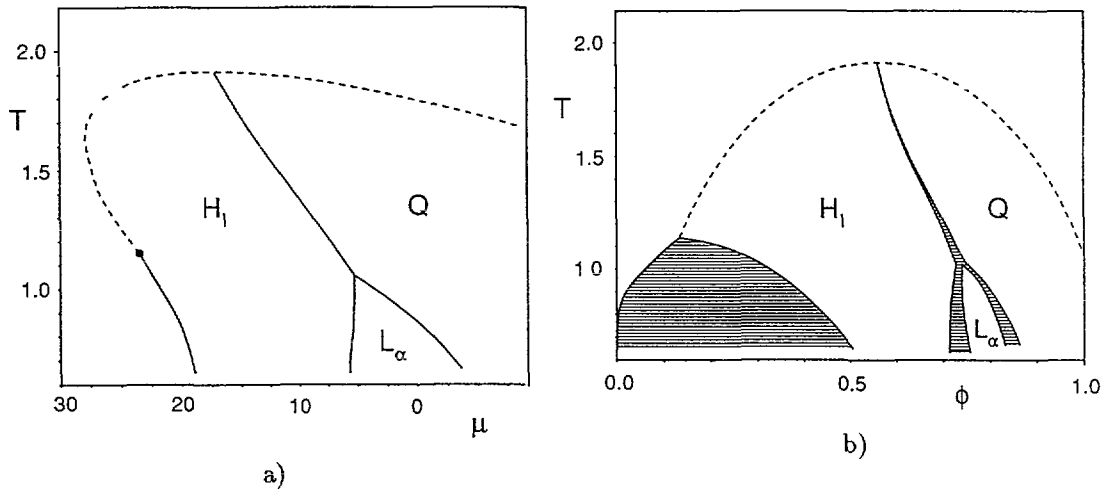

Fig. 11. — Phase diagram for the Flory free energy with the parameters $\alpha_1 = -10$, $\alpha_2 + \alpha_4 = 10$, $\beta_1 = 10$, $\gamma = 30$, $M = 20$, $a_2 = 1$, $b_2 = -10$, $c_2 = 17/12$, $c_4 = 1$. (a) Temperature *vs.* chemical potential plane. Phase transitions along dashed lines are second order. The tricritical point is marked by a dot (•). (b) Temperature *vs.* amphiphile concentration plane.

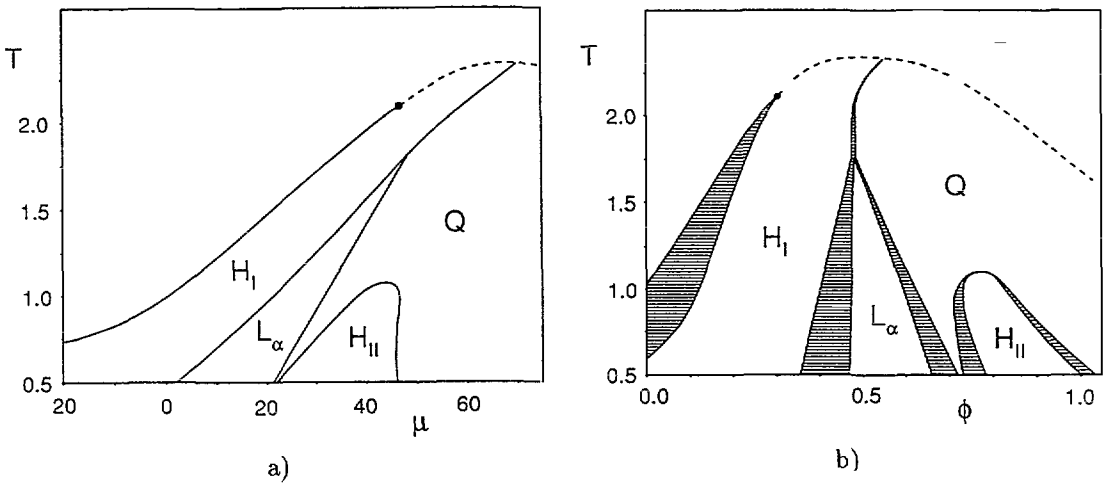

Fig. 12. — Phase diagram for the Landau free energy with the parameters $\alpha_1 = -10$, $\alpha_2 + \alpha_4 = 10$, $\beta_1 = 10$, $\gamma = 30$, $M = 20$, $a_2 = 1$, $b_2 = -10$, and $\tilde{a}_2 = 90$, $\tilde{a}_3 = -186$, $\tilde{a}_4 = 264$, $\tilde{a}_5 = -197$, $\tilde{a}_6 = 65$, $\tilde{b}_2 = 15/4$, $\tilde{b}_4 = 1$, $\tilde{c}_1 = -5$, $\tilde{c}_2 = 2.5$. (a) Temperature *vs.* chemical potential plane. Phase transitions along dashed lines are second order. The tricritical point is marked by a dot (•). (b) Temperature *vs.* amphiphile concentration plane.

Thus, all types of ordered phases observed in experiments are present in our model. Moreover, with increasing surfactant concentration, we see exactly the sequence of phases

$$\text{hexagonal} \rightarrow \text{lamellar} \rightarrow \text{cubic} \rightarrow \text{inverse hexagonal} \tag{22}$$

which is observed experimentally [3, 26, 28]. For certain values of the parameters, some of these phases may be missing in the sequence. We have also seen in figure 12 that re-entrant behavior is possible.

The phase sequence (22) is also expected [26, 28] from general arguments based on the elastic properties of surfactant monolayers. We will come back to such an interfacial model in section 6 below.

5. Micelles and bilayers.

We have shown in section 2 that the tendency of amphiphiles to self-assemble into various ordered structures is already present as short-range correlations in disordered phases. The correlations which were calculated in section 2 are due to *small* fluctuations of the order parameter around its average. However, there are also *large* fluctuations in the disordered phase, amphiphiles which have assembled into metastable aggregates of spherical or cylindrical shape. To calculate the size and shape of these micelles, we are looking for order parameter configurations of spherical or cylindrical symmetry. If we assume that the amphiphile points outwards radially, we have

$$\begin{aligned} \phi(\mathbf{r}) &= \phi(r) \\ \tau(\mathbf{r}) &= \tau(r)\hat{\mathbf{r}} \end{aligned} \tag{23}$$

where $\hat{\mathbf{r}} = \mathbf{r}/r$ is the unit radial vector in two dimensions for cylindrical, and in three dimensions for spherical micelles. We then use the same approach as used in the last section for the ordered phases, to write the order parameter profiles $\phi(r)$ and $\tau(r)$ as a series of linearly independent functions. For a single micelle, both order parameters must approach their bulk values in the homogeneous, disordered phase *exponentially* for distances far from the center of the micelle. Thus we make the ansatz

$$\begin{aligned} \phi(r) &= \phi_0 + w(r) \sum_{n=0}^{N} a_n r^{2n} \\ \tau(r) &= w(r) \sum_{n=0}^{N} b_n r^{2n+1} \end{aligned} \tag{24}$$

where the weight function $w(r)$ is taken to be

$$w(r) = \frac{1}{\cosh(r/\xi)} \tag{25}$$

and ξ is the bulk correlation length (which we take as a free variational parameter). The same ansatz can also be used for bilayers with planar geometry. For the numerical calculations we have used $N = 4$, so that we have a total of 11 variational parameters.

The free energies of spherical and cylindrical micelles, and of bilayers are shown in figure 13 for temperature $T = 1$ of figure 12 as a function of the average surfactant concentration, ϕ_0, far away from the aggregate. For small surfactant concentration, spherical micelles become metastable first, at a concentration $\phi_0 \simeq -0.0148$, then stable at $\phi_0 \simeq -0.0027$. At higher

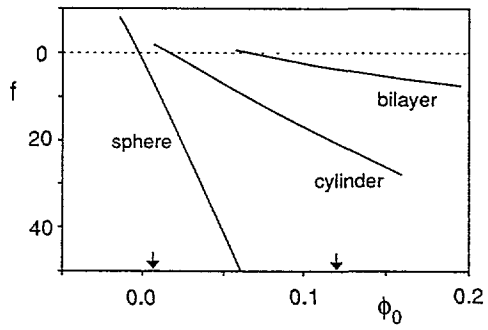

Fig. 13. — Free energies, f, of bilayers (per unit area), and of cylindrical (per unit length) and spherical micelles, as a function of the average surfactant concentration ϕ_0, for $T = 1$ and the Landau free energy (4), (5). The parameters are the same as in figure 12. The arrows indicate the width of the two-phase coexistence region between homogeneous and hexagonal phase.

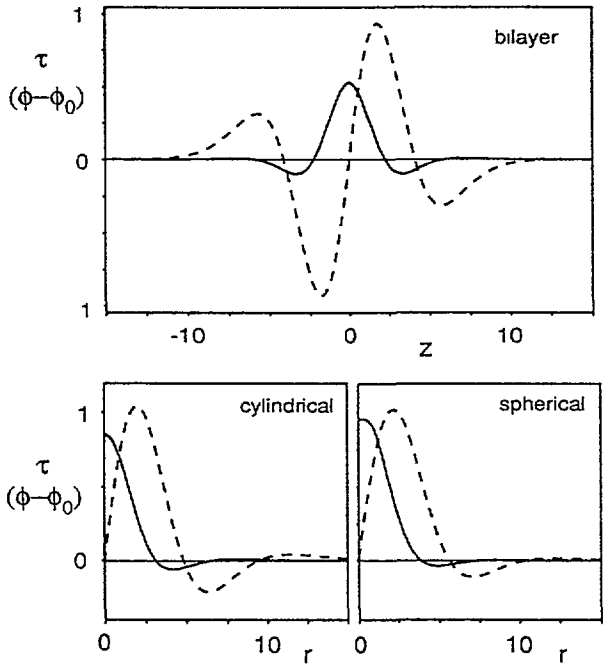

Fig. 14. — Order parameter profiles for bilayers ($\phi_0 \simeq 0.0571$), and for cylindrical ($\phi_0 \simeq 0.0064$) and spherical ($\phi_0 \simeq -0.0148$) micelles, at $T = 1$ and the Landau free energy (4), (5). The parameters are the same as in figures 12 and 13.

concentrations, the same happens for the cylindrical micelles, and at even higher concentrations for bilayers. The order parameter profiles for micelles and bilayers at their limit [29] of metastability are shown in figure 14.

We see from figures 12 and 13 that the concentration $\phi_0 \simeq 0.0062$ of the homogeneous phase at coexistence with the hexagonal phase is *larger* than the concentration where spherical micelles become stable. This indicates that there must be another phase, consisting of packed spherical micelles, which is stable at low concentrations. Indeed, the Fourier analysis (21) reveals that in fact a body-centered cubic (bcc) phase is stable in a narrow range between the homogeneous and the hexagonal phase [30]. The stability of this bcc phase, and of other cubic phases, will be studied in more detail in the future.

6. Membrane elasticity.

The basic input of 'interfacial' models [11, 12, 14] of binary surfactant mixtures is the bending elasticity of surfactant bilayers, which is given by the Helfrich expression [11, 31]

$$\mathcal{H}_{\text{memb}} = \int \mathrm{d}S \left[\sigma + \lambda H + 2\kappa H^2 + \bar{\kappa} K\right] \tag{26}$$

where the integral is over the whole membrane area, $H = \frac{1}{2}(1/R_1 + 1/R_2)$ is the local mean curvature (with the principle radii of curvature, R_1 and R_2), and $K = 1/(R_1 R_2)$ the local Gaussian curvature. The properties of a particular surfactant system enter the theory *via* the elastic coefficients in (26), which are the surface tension σ, the spontantous curvature $H_0 = -\lambda/(4\kappa)$, the bending rigidity κ, and the saddle splay modulus $\bar{\kappa}$. Several attempts have been made to calculate the elastic moduli from microscopic models for a surfactant bilayer or monolayer [32-34]. We want to show here how these elastic moduli can be calculated from our Landau model [35, 36, 19, 37].

We follow the path used in reference [36] and calculate the free energies (per unit area) of a planar surfactant bilayer, and of cylindrical and spherical vesicles of radius R. In all these cases, the order parameter profile which minimizes the free energy functional is given by the solution of the Euler-Lagrange equations

$$\begin{aligned} &\frac{1}{2}\frac{\partial}{\partial\phi}U(\phi,\tau^2) - \beta_1\nabla^2\phi - \frac{1}{2}\gamma\nabla\cdot\tau = 0 \\ &\frac{1}{2}\frac{\partial}{\partial\tau_\alpha}U(\phi,\tau^2) - (\alpha_1-\alpha_3)\partial_\alpha(\nabla\cdot\tau) + \alpha_2(\nabla^2)^2\tau_\alpha - \alpha_3\nabla^2\tau_\alpha \\ &\qquad\qquad + \alpha_4\partial_\alpha\nabla^2(\nabla\cdot\tau) + \frac{1}{2}\gamma\partial_\alpha\phi = 0 \end{aligned} \tag{27}$$

For the profile of a planar membrane, with all surfactant molecules oriented perpendicular to the membrane on average, the set of equations (27) has one integral; it can be found by multiplying the first equation with $\tau' = \frac{\mathrm{d}}{\mathrm{d}z}\tau$, the second with $\phi' = \frac{\mathrm{d}}{\mathrm{d}z}\phi$, and adding the two equations together, with the result

$$(\alpha_2+\alpha_4)(2\tau'\tau''' - \tau''^2) - \alpha_1\tau'^2 - \beta_1\phi'^2 + U(\phi,\tau^2) = \text{const} \tag{28}$$

This equation can be used to write the free energy (3) of the planar membrane (per unit area), with $\tau = \bar{\tau}(z)\hat{\mathbf{z}}$ and $\phi = \bar{\phi}(z)$, where $\hat{\mathbf{z}}$ is the unit vector in the z-direction, in the form

$$\sigma = \frac{F}{A} = \int \mathrm{d}z \left[2\alpha_1\bar{\tau}'^2 + 4(\alpha_2+\alpha_4)\bar{\tau}''^2 + 2\beta_1\bar{\phi}'^2 + \gamma\bar{\tau}\bar{\phi}'\right] \tag{29}$$

which is just the surface tension.

For the cylindrical ($d = 2$) and spherical ($d = 3$) vesicles we again assume that all amphiphiles are locally oriented perpendicular to the membrane on average, i.e. $\tau = \tau(r)\hat{\mathbf{r}}$ and $\phi = \phi(r)$, where $\hat{\mathbf{r}}$ is again the unit radial vector in cylindrical or spherical coordinates. In this case we have

$$\begin{aligned} \nabla \cdot \tau &= \frac{d-1}{r}\tau + \frac{\mathrm{d}}{\mathrm{d}r}\tau \\ \nabla(\nabla \cdot \tau) = \nabla^2\tau &= \left[-\frac{d-1}{r^2}\tau + \frac{d-1}{r}\frac{\mathrm{d}}{\mathrm{d}r}\tau + \frac{\mathrm{d}^2}{dr^2}\tau\right]\hat{\mathbf{r}} \end{aligned} \tag{30}$$

so that the free energy density, $f_c \equiv F/A$, reads

$$\begin{aligned} f_c = R^{-(d-1)} \int_0^\infty \mathrm{d}r r^{d-1} \Bigg[& \alpha_1 \left(\frac{d-1}{r}\tau + \tau'\right)^2 + (\alpha_2 + \alpha_4)\left(-\frac{d-1}{r^2}\tau + \frac{d-1}{r}\tau' + \tau''\right)^2 \\ & + \beta_1 \phi'^2 + \gamma\tau\phi' + U(\phi, \tau^2)\Bigg] \end{aligned} \tag{31}$$

We want to determine the elastic moduli in the Helfrich expression (26) by expanding the free energy of cylinders and spheres in powers of the inverse radius R^{-1}, and comparing coefficients. In order to proceed analytically, we assume that the order parameter profiles in the curved geometries can be expanded in a power series in R^{-1} around the planar profile, so that

$$\tau(r) = \bar{\tau}(r - R) + O(R^{-1}), \qquad \phi(r) = \bar{\phi}(r - R) + O(R^{-1}). \tag{32}$$

It has been shown recently that for a *single* order parameter Landau theory the elastic moduli can be obtained by using only the leading terms in (32), i.e. by replacing the full profile by the planar profile, with very good results [36, 38]. Therefore, we will proceed here with the same approximation. We can now replace r by $(r - R)$ as the variable of integration, and use the integral (28) to eliminate $U(\bar{\phi}, \bar{\tau}^2)$. This leads to the free energy integral

$$\begin{aligned} f_c = R^{-(d-1)} \int_{-R}^\infty \mathrm{d}r (R + r)^{d-1} \Bigg[& \alpha_1 \left(\frac{d-1}{R+r}\bar{\tau} + \bar{\tau}'\right)^2 \\ & + (\alpha_2 + \alpha_4)\left(-\frac{d-1}{(R+r)^2}\bar{\tau} + \frac{d-1}{R+r}\bar{\tau}' + \bar{\tau}''\right)^2 \\ & + \beta_1 \bar{\phi}'^2 + \gamma\bar{\tau}\bar{\phi}' + \left\{-(\alpha_2 + \alpha_4)(2\bar{\tau}'\bar{\tau}''' - \bar{\tau}''^2) + \alpha_1 \bar{\tau}'^2 + \beta_1 \bar{\phi}'^2\right\}\Bigg] \end{aligned} \tag{33}$$

For large R, we can extend the lower boundary of integration from $-R$ to $-\infty$, since this will only give contributions of order $\mathrm{e}^{-R/\xi}$, where ξ is the bulk correlation length of the interior phase. All what is left to be done is to expand the integrand of equation (33) in a power series in R^{-1} A straightforward calculation then gives for cylinders

$$f_{\mathrm{cyl}} = \sigma + \frac{1}{R}\int_{-\infty}^\infty \mathrm{d}r\, r\, p_s(r) + \frac{1}{R^2}\int_{-\infty}^\infty \mathrm{d}r \left[\alpha_1 \bar{\tau}^2 + 3(\alpha_2 + \alpha_4)\bar{\tau}'^2\right] + O(R^{-3}) \tag{34}$$

and for spheres

$$\begin{aligned} f_{\mathrm{sph}} = \sigma & + \frac{2}{R}\int_{-\infty}^\infty \mathrm{d}r\, r\, p_s(r) \\ & + \frac{1}{R^2}\int_{-\infty}^\infty \mathrm{d}r\, r^2\, p_s(r) + \frac{1}{R^2}\int_{-\infty}^\infty \mathrm{d}r \left[2\alpha_1 \bar{\tau}^2 + 4(\alpha_2 + \alpha_4)\bar{\tau}'^2\right] + O(R^{-3}) \end{aligned} \tag{35}$$

where

$$p_s(r) = 2\alpha_1 \bar{\tau}'^2 + 4(\alpha_2 + \alpha_4)\bar{\tau}''^2 + 2\beta_1 \bar{\phi}'^2 + \gamma \bar{\tau} \bar{\phi}' \tag{36}$$

A comparison of our results (34) and (35) with the Helfrich expression (26) leads to the identification

$$\sigma = \int_{-\infty}^{\infty} \mathrm{d}r \; p_s(r) \tag{37a}$$

$$\lambda = 2 \int_{-\infty}^{\infty} \mathrm{d}r \; r \; p_s(r) \tag{37b}$$

$$\kappa = 2 \int_{-\infty}^{\infty} \mathrm{d}r \left[\alpha_1 \bar{\tau}^2 + 3(\alpha_2 + \alpha_4)\bar{\tau}'^2\right] \tag{37c}$$

$$\bar{\kappa} = \int_{-\infty}^{\infty} \mathrm{d}r \; r^2 \; p_s(r) - 2 \int_{-\infty}^{\infty} \mathrm{d}r \left[\alpha_1 \bar{\tau}^2 + 4(\alpha_2 + \alpha_4)\bar{\tau}'^2\right] \tag{37d}$$

This result for the elastic moduli of surfactant bilayers shows strong similarities with the result for the surfactant monolayers in oil-water-surfactant mixtures derived in reference [36]. In particular, we find that the surface tension σ and the spontanous curvature modulus λ are the moments of the stress profile $p_s(z)$, as expected from general arguments on the elasticity of interfaces [39]. However, there are important differences. First, we see that the second moment of the stress profile cannot be written as a linear combination of κ and $\bar{\kappa}$. We conclude that this is a coincidence in the single order parameter model studied in reference [36]. Second, since α_1 can be negative, it is not obvious that κ must always be positive in the present model. Finally we want to emphasize that our result (37c) for the bending rigidity depends mainly on orientation-dependent properties of the amphiphile (determined by the interaction constants α_1, α_2 and α_4), whereas the water-amphiphile interaction enters only *via* the form of the order parameter profile.

7. Summary and discussion.

We have introduced a two order parameter Ginzburg-Landau model for aqueous surfactant solutions. The amphiphile concentration is described by a scalar, the orientational degrees of the amphiphile by a vector order parameter. We have shown that this model describes a wide range of phenomena in binary water-surfactant mixtures. In the disordered phase, the tendency of the amphiphiles to self-assemble already shows up in the correlation functions and scattering intensities. Micelles exist as metastable aggregates at low surfactant concentrations. At higher surfactant concentrations, several ordered lyotropic phases have been found, with the generic phase sequence

hexagonal → lamellar → cubic → inverse hexagonal.

Our model has also been used to derive expressions for the elastic bending moduli of amphiphilic bilayers in terms of the order parameter profiles of the *flat* interface.

All these results are in good qualitative agreement with experimental observations. However, it would be nice if more stringent comparisons could be made. The concentration profiles of lyotropic phases could be determined by scattering techniques [4, 40, 41], for example, and compared with those shown in figures 7-10. Or, if the order parameter profiles [42, 43] of a bilayer *and* its elastic constants [44, 45] could be measured, a test of equation (37) for the elastic moduli would be possible. We want to emphasize that the *simultanous* measurement of phase behavior, scattering intensity, elastic constants, etc. for the *same* system would in

our view be most promising for an experimental test of our theory. Here, the system $C_{12}E_8$ plus water seems to be an ideal candidate, because not only its phase diagram [3,46] shows remarkable similarities with our figure 6, but also the scattering intensity in the disordered phase shows the behavior with increasing amphiphile concentration as discussed in section 3.

A generalization of our Landau model to ternary mixtures of water, surfactant and oil, is straightforward. It requires a third scalar order parameter for the oil concentration [19, 37]. With such a generalized model, the crossover from binary to ternary mixtures could be studied, which has received little attention so far.

Acknowledgements.

This work was supported in part by the Deutsche Forschungsgemeinschaft through Sonderforschungsbereich 266. We acknowledge many helpful discussions with Stefan Zschocke.

Appendix A.

Mean-field entropy.

To derive the entropy in the mean-field approximation, we divide space into cells of equal size, such that each cell is occupied by exactly one amphiphile, or by no amphiphile at all. We can then introduce a vector variable $\mathbf{s}_i$ for each cell i, which describes both the occupation of the cell and the orientation of an amphiphile, with $\mathbf{s}_i^2 \in \{0, 1\}$, where $\mathbf{s}_i^2 = 0$ is a cell with no amphiphile. In the mean-field approximation, the full density matrix is replaced by a product of single site matrices

$$w_i = \frac{1}{Z_i} \mathrm{e}^{-\beta \mathbf{h}_i \cdot \mathbf{s}_i - \beta \Delta_i \mathbf{s}_i^2} \tag{A1}$$

with the partition function Z_i, and $\beta = 1/k_B T$. The effective fields $\mathbf{h}_i$ and Δ_i are determined from the single site averages

$$\begin{aligned} \phi_i &\equiv < \mathbf{s}_i^2 > = -\beta^{-1} \frac{\partial \ln Z_i}{\partial \Delta_i}, \\ \tau_i &\equiv < \mathbf{s}_i > = -\beta^{-1} \frac{\partial \ln Z_i}{\partial \mathbf{h}_i} \end{aligned} \tag{A2}$$

With

$$\begin{aligned} Z_i &= 1 + \int_0^{2\pi} \mathrm{d}\varphi \int_0^{\pi} \mathrm{d}\vartheta \sin\vartheta \ \mathrm{e}^{-\beta h_i \cos\vartheta - \beta \Delta_i} \\ &= 1 + 4\pi \mathrm{e}^{-\beta \Delta_i} \frac{\sinh \beta h_i}{\beta h_i} \end{aligned} \tag{A3}$$

we obtain

$$\begin{aligned} \phi_i &= \frac{4\pi}{Z_i} \mathrm{e}^{-\beta \Delta_i} \frac{\sinh \beta h_i}{h_i} \\ \tau_i &= -\phi_i [\coth \beta h_i - \frac{1}{\beta h_i}] \frac{\mathbf{h}_i}{h_i} \end{aligned} \tag{A4}$$

and

$$Z_i = \frac{1}{1 - \phi_i}. \tag{A5}$$

From these results, we can calculate the entropy S as a function of the averages ϕ_i and τ_i,

$$S = \sum_i [\mathbf{h}_i \cdot \tau_i + \Delta_i \phi_i + \ln Z_i] . \tag{A6}$$

Since we cannot invert (A4) exactly, we expand the right-hand side in a power series, and invert iteratively, with the result

$$\beta h_i = -3\tilde{\tau}_i - \frac{9}{5}\tilde{\tau}_i^3 + .. \tag{A7}$$

where $\tilde{\tau} = \tau/\phi$. Inserting h_i from (A7) and Δ_i from (A4) into equation (A6), and also expanding $\ln[\sinh \beta h_i/(\beta h_i)]$, we finally obtain

$$S = -\sum_i [\phi_i \ln \phi_i + (1-\phi_i)\ln(1-\phi_i) + \phi_i(c_2\tilde{\tau}_i^2 + c_4\tilde{\tau}_i^4 + ..)] \tag{A8}$$

where $c_2 = 3/2$, $c_4 = 33/20$. Here, we have included the fourth order term in the expansion in $\tilde{\tau}$ to insure thermodynamic stability. The numerical values of c_2 and c_4 are of little importance, since they can be changed by a rescaling of $\tilde{\tau}$. We will therefore treat c_2 and c_4 as free parameters of the model.

References

[1] *Physics of Amphiphilic Layers*, edited by J. Meunier, D. Langevin, and N. Boccara, Springer Proceedings in Physics, Vol.21 (Springer, Berlin 1987).

[2] *Modern Ideas and Problems in Amphiphilic Science*, edited by W.M. Gelbart, D. Roux, and A. Ben-Shaul, to be published.

[3] G.J.T. Tiddy, Phys. Rep. **57**, 1 (1980).

[4] V. Luzzati, in *Biological Membranes*, edited by D. Chapman (Academic Press, New York, 1968).

[5] L.E. Scriven, Nature **263**, 123 (1976).

[6] J. Charvolin, J. Phys. France **46**, C3-173 (1985).

[7] J.W. Halley and A.J. Kolan, J. Chem. Phys. **88**, 3313 (1988).

[8] G. Gompper and M. Schick, Chem. Phys. Lett. **163**, 475 (1989).

[9] M.W. Matsen and D.E. Sullivan, Phys. Rev. A**41**, 2021 (1990).

[10] K.A. Dawson and Z. Kurtović, J. Chem. Phys. **92**, 5473 (1990).

[11] W. Helfrich, Z. Naturforsch. **28c**, 693 (1973).

[12] D. Huse and S. Leibler, J. Phys. France **49**, 605 (1988).

[13] D.M. Anderson, H.T. Davis, L.E. Scriven, and J.C.C. Nitsche, Adv. Chem. Phys. **77**, 337 (1990), and references therein.

[14] M.E. Cates, D. Roux, D. Andelman, S.T. Milner, S.A. Safran, Europhys. Lett. **5**, 733 (1988).

[15] See, e.g. R.E. Goldstein, J. Chem. Phys. **84**, 3367 (1986); M. Borkovec, J. Chem. Phys. **91**, 6268 (1989), and references therein.

[16] M. Teubner and R. Strey, J. Chem. Phys. **87**, 3195 (1987).

[17] G. Gompper and M. Schick, Phys. Rev. Lett. **65**, 1116 (1990).

[18] K. Chen, C. Jayaprakash, R. Pandit, and W. Wenzel, Phys. Rev. Lett. **65**, 2736 (1990).

[19] K. Kawasaki and T. Kawakatsu, Physica A**164**, 549 (1990).

[20] P.-G. de Gennes, *Scaling Concepts in Polymer Physics* (Cornell University Press, Ithaca, New York, 1979).

[21] R.E. Goldstein, J. Chem. Phys. **83**, 1246 (1985), and references therein.
[22] M.E. Fisher and B. Widom, J. Chem. Phys. **50**, 3756 (1969); J. Stephenson, J. Math. Phys. **11**, 420 (1970).
[23] G. Gompper and M. Schick, Phys. Rev. Lett. **62**, 1647 (1989).
[24] Since $\nabla \times \tau \equiv 0$, the phase diagrams do not depend explicitly on the value of α_3. However, it has to be kept in mind that $\alpha_3 > 0$ has to be large enough for the correlation function $< \tau_z(0)\tau_z(x) >$ to decay monotonically in the disordered phase, compare the discussion after Eq.(19).
[25] The position of second order phase transitions from the disordered phase to a spatially modulated phase can be located by the divergence of the scattering intensity (13).
[26] J.M. Seddon, Biochimica et Biophysics Acta **1031**, 1 (1990), and references therein.
[27] There is some ambiguity in the definition of a 'bicontinuous' phase in our model. When constant concentration surfaces, with $\phi(\mathbf{r}) = \phi^*$, are used to divide space into water-rich and amphiphile-rich regions, the phase shown in figure 10 is bicontinuous for $0.58 \lesssim \phi^* \lesssim 0.80$, but is not for $0.25 \lesssim \phi^* \lesssim 0.57$. Other definitions of a dividing surface, like $\nabla \cdot \tau = 0$, are also possible.
[28] S.M. Gruner, J. Phys. Chem. **93**, 7562 (1989).
[29] The limits given here are of course only upper bounds for the metastability of micelles and bilayers.
[30] At $T = 1$, the concentrations of the homogeneous and the bcc phase at coexistence are $\phi_0 \simeq -0.020$ and $\phi_0 \simeq 0.060$, respectively.
[31] Our expression (26) agrees with the usual form of the Helfrich Hamiltonian for *tensionless* monolayers, $\mathcal{H} = \int dS[2\kappa(H - H_0)^2 + \bar{\kappa}K]$ with $H_0 = 1/R_0$, in the special case $\sigma = 2\kappa R_0^{-2}$.
[32] I. Szleifer, D. Kramer, A. Ben-Shaul, D. Roux, and W.M. Gelbart, Phys. Rev. Lett. **60**, 1966 (1988).
[33] The effect of electrostatic interactions on the curvature elasticity have been studied by H.N.W. Lekkerkerker, Physica A**159**, 319 (1989); Physica A**167**, 384 (1990); D. Bensimon, F. David, S. Leibler, and A. Pumir, J. Phys. France **51**, 689 (1990); P. Pincus, J.-F. Joanny, and D. Andelman, Europhys. Lett. **11**, 763 (1990); B. Duplantier, R.E. Goldstein, V. Romero-Rochín, and A.I. Pesci, Phys. Rev. Lett. **65**, 508 (1990).
[34] Estimates of the bending moduli in polymer systems have been discussed by S.T. Milner and T.A. Witten, J. Phys. France **49**, 1951 (1988); Z.G. Wang and S.A. Safran, J. Phys. France **51**, 185 (1990); J. Chem. Phys. **94**, 679 (1991).
[35] R.K.P. Zia, Nucl. Phys. B**251** [FS13], 676 (1980).
[36] G. Gompper and S. Zschocke, Europhys. Lett. **16**, 731 (1991).
[37] T. Kawakatsu and K. Kawasaki, Physica A**167**, 690 (1990).
[38] With the elastic moduli calculated this way, the Helfrich free energy (26) was found to agree very well with the free energy obtained from the solution of the Euler-Lagrange equations.
[39] W. Helfrich, in *Physics of Defects*, edited by R. Balian, M. Kléman, J.-P. Poirier (North-Holland, 1981).
[40] J.M. Seddon, J.L. Hogan, N.A. Warrender, and E. Pebay-Peyroula, Progr. Colloid Polym. Sci **81**, 189 (1990).
[41] J.M. Seddon, E.A. Bartle, and J. Mingins, J. Phys. Condens Matter **2**, SA285 (1990).
[42] P.S. Pershan, Coll. Phys. **50**, C7-1 (1989).
[43] G. Cevc, W. Fenzl, and L. Sigl, Science **249**, 1161 (1990).
[44] L.T. Lee, D. Langevin, and B. Farnoux, Phys. Rev. Lett. **67**, 2678 (1991).
[45] J.M. di Meglio and P. Bassereau, J. Phys. II France **1**, 247 (1991).
[46] V. Degiorgio, M. Corti and L. Cantú, Chem. Phys. Lett. **151**, 349 (1988).